minerals

MDPI

Article

Bioavailability of Colloidal Iron to Heterotrophic Bacteria in Sediments, and Effects on the Mobility of Colloid-Associated Metal(loid)s

Malgorzata Grybos *, Delphine Masson, Pauline Gorgeon, Patrice Fondanèche, Nicolas Martin, Fabrice Dupuy, Emmanuel Joussein and Valentin Robin *

E2Lim (UR 24 133), Université de Limoges, 123 Avenue Albert Thomas, CEDEX, 87060 Limoges, France; delphine.masson@unilim.fr (D.M.); pauline.gorgeon@etu.unilim.fr (P.G.); patrice.fondaneche@unilim.fr (P.F.); nicolas.martin@unilim.fr (N.M.); fabrice.dupuy@unilim.fr (F.D.); emmanuel.joussein@unilim.fr (E.J.)

* Correspondence: malgorzata.grybos@unilim.fr (M.G.); valentin.robin@unilim.fr (V.R.)

Abstract: The submicrometric fraction of surface sediments that accumulate in the bottom of dam reservoirs represent important sources of nutrients and contaminants in freshwater systems. However, assessing their stability in the presence of sediment bacteria as well as their bioavailability in the sediment remains poorly understood. We hypothesized that sediment's bacteria are able to extract nutrients from sedimentary colloids (<1 µm fraction) and thus contribute to the release of other colloid-associated elements to water. Experiments were performed under laboratory conditions, using the submicrometric fractions of sediments recovered from two dam reservoirs (in calcareous and crystalline granitic contexts) and two heterotrophic bacteria (Gram-negative *Pseudomonas* sp. and Gram-positive *Mycolicibacterium* sp.). The results demonstrated that bacteria were able to maintain their metabolic activity (the acidification of the growth medium and the production of organic ligands) in the presence of colloids as the sole source of iron (Fe) and regardless of their chemical composition. This demonstrates that bioavailable Fe, aside from ionic forms, can also occur in colloidal forms. However, the bacteria also catalyzed the release of potentially toxic metallic elements (such as Pb) associated with colloids. These results help improve our understanding of the processes that influence contaminants' mobility in the ecosystems as well as provide an important insight into current research evaluating the bioavailability of different forms of nutrients.

Keywords: bio-dissolution; bio-weathering; colloids; bacteria; sediments; metals; dam reservoir; inorganic contaminants; nutrients; iron

Citation: Grybos, M.; Masson, D.; Gorgeon, P.; Fondanèche, P.; Martin, N.; Dupuy, F.; Joussein, E.; Robin, V. Bioavailability of Colloidal Iron to Heterotrophic Bacteria in Sediments, and Effects on the Mobility of Colloid-Associated Metal(loid)s. *Minerals* **2022**, *12*, 812. https://doi.org/10.3390/min12070812

Academic Editors: Anna Panyushkina and Maxim Muravyov

Received: 24 May 2022
Accepted: 23 June 2022
Published: 25 June 2022

1. Introduction

The input of nutrients and/or contaminants into surface freshwater and their bioavailability is of great ecological importance for these ecosystems. Despite the regulation of anthropogenic inputs of undesirable elements into surface waters, many lakes and reservoirs do not show the expected environmental improvement; for example, in 2015 about 40% of surface water in Europe still had an ecological status that was below 'good' [1]. The delayed improvement of water quality in some cases is related to the release of undesirable elements from the sediments [2,3]. Sediments accumulated in the bottom of the lakes and reservoirs hold an important stock of nutrients [4] and various types of metallic and organic contaminants [5]. Moreover, bottom sediments are regarded as geochemical reactors and regulators that mediate and influence the fluvial transport of nutrients and contaminants along the land–ocean continuum, as well as their transformation and thus their biogeochemical cycle [6].

Recently, there has been a growing interest in the characterization of the fine fraction of the sediments accumulated in aquatic ecosystems, particularly those that can be resuspended during sediment bioturbation, turbulent flows associated with seasonal flooding or

storms, or during human activities (dredge disposal, dredging, dam management) [7–10]. Up-to-date studies conducted on sediments accumulated in dam reservoirs in crystalline catchment areas have revealed that water-dispersible submicrometric fractions of sediments (<1 µm, later referred to as sedimentary colloids) are components inherent to bottom sediments, not only in the lacustrine area favoring the deposition of the finest particles, but also in the upstream, more riverine part of the reservoir [8,10,11]. It was also demonstrated that sedimentary colloids contain nutrients (P, organic C, Fe, Ca, Mg, etc.) and metallic (metalloid) contaminants [7,8,10,11]. Sedimentary colloids, as highly reactive and potentially mobile fractions of sediments, may play an important role in maintaining the balance of nutrients and contaminants in both sediment and water, and thus affect the quality of the overlying water and downstream rivers [9]. Additionally, the co-occurrence of colloids and microorganisms in the sediment or the water column makes the colloid-associated nutrients potentially bioavailable [12] and colloid-associated contaminants potentially soluble. Therefore, the bio-sequestration of nutrients from the colloids can lead to their solubilization and the solubilization of related elements (including contaminants, if any). However, determining the (bio-)availability of an element associated with the colloids in a sedimentary environment is challenging because the microorganisms are in contact with both the dissolved and the solid phases, and can in principle sequester nutrients from both compartments. Moreover, the distribution of an element between dissolved and solid phases depends mainly on the partitioning behavior or binding strength of the element to the sediment. This distribution is strongly influenced by the physico-chemical properties of the particles (e.g., size, chemical composition, etc.) and varies depending on (i) the type and speciation of elements, (ii) the prevailing physico-chemical conditions in the water (pH, redox potential, temperature, the presence of ligands and competing elements, etc.) and (iii) the organism considered (e.g., from micro- to macro-organisms, between different bacterial strains, etc.) [13–15]. In addition, biological activity itself strongly influences the physico-chemical environment in the sediment, and in turn, affects the bioavailability of an element (due to pH change, the reduction or oxidation of redox sensible elements, the depletion of oxygen and the production or transformation of organic compounds) [15]. Therefore, to improve our understanding of the processes and factors that control the mobility of nutrients and contaminants in the ecosystem, it is important to evaluate the stability of sedimentary colloids in the presence of indigenous bacteria and the bioavailability of colloid-related elements.

Several techniques are available to evaluate the bioavailability of elements in sediments. Among the most common ones are sequential or selective chemical extraction [16–18], thin-film diffusive gradient techniques (DGT) [19–21], or bio-concentration using living biota, mainly filter-feeding organisms [22]. However, the bioavailability of colloid-associated elements to bacteria, and the role of biochemical processes involved specifically at the bacteria–colloid–water interface, are not assessed by means of such methodologies. Additionally, in experiments designed to incubate colloidal suspension with bacteria, the aggregation and flocculation of uncontrolled colloids and/or colloid adsorption onto bacterial cells may occur, thus decreasing the surface area of colloids available for interactions with bacteria and/or with the solution. In such situation, it is difficult to correctly compare colloid stability under biotic and abiotic conditions. Moreover, the characterization of interactions between bacteria and sedimentary colloids is challenging due to the difficulty in mimicking a solid mineral environment, which is poor in organic matter and has controlled nutrient content. The solid agar culture media used for bacterial cultivation are based on organic polymers and consist of a range of directly bioavailable nutrients. Therefore, a full control of the bioavailable nutrients content for the microorganisms is not possible because the bacteria can feed on the agar instead of colloids. One possible approach to investigating the bioavailability of colloids is to culture bacteria on porous, inorganic colloid-doped gel [23]. In such an approach, bacteria stay on the gel and either directly interact with colloids at the gel surface and/or produce metabolites that can be transported through the gels' porosity and interact with immobilized particles. Thus, more fundamental research

and experimental data using both well characterized micro-organisms and natural sedimentary colloids, at the same time, are needed as (i) metals bioavailability assessment without micro-organisms present in the system (e.g., bioavailability assessed from sequential extraction) cannot fully describe the biochemical processes involved at the bacteria-colloid-water interface and (ii) data of colloid bio-weathering experiments are scarce, as most of the available studies are performed on larger (and less chemically reactive) size fraction, or monomineralic fractions not representative of natural (polyphasic) colloids.

The present study aimed to evaluate the ability of indigenous bacteria (Gram-negative, *Pseudomonas* sp., and Gram-positive, *Mycolicibacterium* sp.) to extract nutrients from sedimentary colloids and their potential contribution to colloid dissolution and the release of colloid-bound metallic elements (Fe, Mn, Pb, Cr and As). In order to avoid the aggregation of colloids or their adsorption on bacterial cells, and to control nutrient input, colloids were embedded in a stable, porous, TEOS-derived silica gel (HSG) [23] prior to inoculation. Our results unravel the capability of two strains of bacteria to increase the release of iron from colloids to the solution, which also implies the release of potentially toxic elements (e.g., Pb).

2. Materials and Methods

2.1. Sediment Sampling and Characteristics

Surface sediments (up to 10 cm deep) from two dam reservoirs were collected in Champsanglard (CHA, latitude of 46.2604, longitude of 1.87743) and in L'Escourou (LSC, latitude of 44.6650, longitude of 0.3480) (Nouvelle Aquitaine region, France) using Ekman stainless steel grabs in the reservoirs' deepest parts (12 m and 14.3 m in depth, respectively). Wet sediments were transported in plastic bottles and stored at 3 °C until further treatments. Those locations were selected because the watersheds' display contrasted lithology, with a crystalline magmatic and a sedimentary calcareous substratum for CHA and LSC, respectively. The land use of each watershed also differs; the percentage of agricultural land, artificial surfaces and forests were, respectively, 85%, 0% and 15% for LSC and 66%, 4% and 30% for CHA. Sediments were analyzed for metal(loid) content by XRF (ED-XRF Spectro-XEPOS, Xep05, SPECTRO Analytical Instruments, Kleve, Germany) after drying (ambient temperature) and milling. The CHA sediment was more Si and Fe-rich, while the LSC sediment displayed higher Ca content. The pH values of sediments were quite different along 1 pH unit; as expected, the pH values were more acidic for sediments derived from magmatic rocks (CHA's pH = 6.5) than for sediments derived from carbonates (LSC's pH = 7.5) (NF ISO 10390 procedure). C and N elemental analyses were carried out by means of a Thermo Fisher 2000 elemental analyzer. The total sedimentary P content was measured by a spectroscopic method at 880 nm after sediment calcination at 450 °C (3 h) and digestion (16 h) in HCl 3.5 M (VWR Prolabo AnalaR Normapur) [24,25]. The grain size distribution was measured using a Mastersizer 3000 laser analyzer (Malvern Panalytical, Malvern, UK) after dispersion in water. Briefly, CHA sediments can be qualified as sandy silt and LSC sediment can be qualified as silt. The physico-chemical characteristics (grain size distribution, chemistry) of the sediments are reported in the Supplementary Materials SI-1 (Tables S1, S2 and Figure S1).

2.2. Colloid Extraction and Characterization

The submicrometric fraction of each sediment was extracted from fresh, wet sediments dispersed in ultrapure water (UPW) by agitation on a rotary agitator (IKA-WERKE KS 501) at 200 rpm for 24 h (1:10 sediments/UPW ratio). The obtained sediment suspension was let to settle for 2 h and then the supernatant was gently pipetted out for colloid separation [11]. The supernatant was pre-filtered at 2.7 µm on a glass fiber membrane (WVR) to remove larger particles and avoid membrane fouling, then filtered at 1 µm on a glass fiber membrane (WVR). Colloid extractions were performed in triplicate, and all membranes prior to the filtration were washed with UPW (20 mL). All chemical analyses were conducted on <1 µm and <0.2 µm fractions. The 0.2–1 µm size fraction's (large

colloids) chemistry was determined by the difference between the 1 µm and <0.2 µm size fractions. Recovered fractions contained biogenic (C_{org}, N, P) and metallic (Pb, As, Cr) elements. Chemical composition was performed in triplicates after acid digestion (HNO_3-HCl) by ICPMS (Agilent 7700x, Agilent Technologies, Santa Clara, CA, USA) using ^{45}Sc and ^{115}In as internal standards. The average limits of quantification (LQ) were 1 µgFe.L^{-1}, 0.07 µgMn.L^{-1}, 0.04 µgAs.L^{-1}, 0.04 µgPb.L^{-1} and 0.03 µgCr.L^{-1}. The analyses of total organic carbon (C_{org}) and nitrogen (N_{tot}) concentrations were determined in triplicates using a TOC-NT analyzer (Analytik Jena, multi-N/C 2100S, Jena, Germany) upon stirring. The LQ of this method is 1 mgC.L^{-1} and 0.25 mgN.L^{-1}. The total phosphorus (P_{tot}) was quantified by spectrophotometry at 880 nm (Agilent 8453 UV-vis spectrometer) using ammonium molybdate and antimony potassium tartrate [24] after persulfate digestion [26]. The LQ of this method is 0.01 mgP.L^{-1}. The size of the recovered colloids (total fraction <1 µm) was determined in triplicate for each replicate using dynamic light scattering at 173° backscatter (ZetaSizer Nano ZS, Malvern Panalytical, Malvern, UK). The mass of the recovered large colloids (0.2–1 µm fraction) was obtained using a gravimetric method after drying (30 °C, 48 h).

2.3. Bacterial Strain Extraction and Identification

Mycolicibacterium sp. was isolated from the CHA sediment, and *Pseudomonas* sp. was isolated from sediments collected from a fracture of a granitic rock near Limoges, France, by mixing the sediment with sterile UPW and spreading it on modified Bushnell–Haas (BHM, see below) solid culture medium (Petri dishes). The bacteria were then purified by successive replications and isolations on new Petri dishes, and later frozen at −20 °C in 20% glycerol until experimentation.

The V3–V4 variable regions of the 16S rRNA gene from isolated strains were directly amplified by PCR using a 2X PCR Master Mix (QIAGEN, Hilden, Germany) with universal 314 Forward (CCTACGGGNGGCWGCAG) and 785 reverse (GACTACHVGGGTATCTAA TCC) oligonucleotides. Each PCR reaction was carried out in 20 µL volume with 10 µM of each primer. PCR amplification was carried out in the Bio Rad MyCycler Thermal Cycler PCR (Bio-Rad, Hercules, CA, USA) as follows: initial denaturation at 95 °C for 2 min, followed by 35 cycles each of 94 °C for 45 s, 53 °C for 45 s and 72 °C for 50 s, and an extension time of 5 min at 72 °C. PCR products, around 400 bp, were purified with a QIAquick PCR purification kit (QIAGEN, Hilden, Germany). The quality of the extracted DNA was analyzed by 2% agarose gel electrophoresis. PCR-amplified DNA fragments (around 500 ng) were sequenced using each previous primer and a BigDye™ Terminator v1.1 Cycle Sequencing Kit (Applied Biosystems, Waltham, MA, USA) according to the manufacturer's instruction. Sequences obtained with the 3500 Dx Genetic Analyzer (Applied Biosystems, Waltham, MA, USA) were analyzed using Applied Biosystems' Sequencher software and submitted to ncbi nucleotide blast for species determination.

The analysis of the 16S rRNA sequences indicated that the Pseudomonas strain could be part of the *Pseudomonas Fluorescence* intrageneric group, since most hits are for species of the *P. fluorescence* lineage (*rhodesia*, *marginalis*, *azotoformans* and *fluorescens*), but there is no possibility of differentiating between them at this time. Regarding the Mycolicibacterium strain, the sequence analysis indicated the species to be *M. moriakaense* or *M. fortuitum*. Thus, due to the difficulty at this stage of characterizing a specific species with the DNA sequence information analyzed (16S hypervariable regions 3 and 4), the two strains will be called *Pseudomonas* sp. and *Mycolicibacterium* sp. hereafter. These particular isolates were used for their capability to be cultivated and to acidify the medium (assessed from pre-feasibility tests).

2.4. Alteration Experiments: The Bacteria-Colloid-Solution Simplified Micro-Ecosystem

2.4.1. Colloid Immobilization in Silica Gel

Prior to incubation experiments, the recovered submicrometric fraction of sediments (containing colloids and dissolved fraction) was embedded in an inorganic, silica-gel

formed by a sol-gel technique [23]. This method permits the avoidance of colloid aggregation and/or adsorption on bacterial cells and the monitoring of solubilized elements' content and bacterial growth. To elaborate a porous silica gel containing homogenously dispersed colloids, one volume of colloidal suspension was gently mixed with 1 volume of concentrated glucose (×10), 1 volume of concentrated (×10) BHM growth medium and seven volumes of silica sol prepared by the acid hydrolysis of tetraethyl orthosilicate (TEOS, 99.99%, Fluka) catalyzed by ultrasound (17 min, Bioblock Scientific 88156, 320 W, Thermo Fisher Scientific, Waltham, MA, USA). Prior to the incorporation of colloids, the pH of silica sol was increased to a pH of 4 using NaOH (0.1 N) to avoid colloid dissolution and then to a pH of 5 to accelerate silica sol condensation. One ml of the obtained hybrid silica sol was then distributed in each well of 48-well flat bottom microplates and left for 30 min at an ambient temperature for gelation. After gently pulling the gels out of the microplate, the obtained 1 mL solid cylinders (hybrid silica gel, HSG) were rinsed in UPW to get rid of the remaining dissolved fraction and were autoclaved (121 °C, 10 min) in UPW to assure their sterility. In the preparation of silica gel without colloids (SG), the volume of colloidal suspension was substituted by the volume of UPW.

2.4.2. Experimental Conditions

All organisms require Fe for life. However, the solubility of Fe in a natural oxygenated environment is very low. Some microorganisms, however, enhance mineral weathering to obtain the necessary nutrients from the mineral lattice to assure their growth. In order to encourage the bacteria to sequester Fe from the colloids, sterilized HSG (containing CHA or LSC colloids) were inoculated with *Pseudomonas* sp. or *Mycolicibacterium* sp. in Fe-deficient BHM growth medium (Test 3, Table 1). An abiotic incubation with HSG used as a control case was also performed to monitor a spontaneous release of elements from colloids (Test 4, Table 1). Additionally, in order to validate the experimental set-up and investigate the biocompatibility of the gels, two additional biotic incubations were performed with dissolved Fe (127 $\mu g \cdot L^{-1}$) and (i) silica gel (Test 2, Table 1) and (ii) without silica gel (Test 1, Table 1). All biotic and abiotic incubations were conducted as follows: three 1 mL doses of HSG were incubated in a 7 mL sterilized growth medium at 20 °C for 1 h to 9 days with gentle, continuous stirring. The incubations were conducted in sterile, flat-bottom, six-well cell-culturing microplates with a lid ensuring gas exchange, under aerobic conditions. The initial pH could change in response to ongoing biogeochemical reactions.

Table 1. Summary of the different experimental conditions used to validate the set up and study the bioavailability and release of elements from sedimentary colloids into the solution under biotic and abiotic conditions.

Test N°	Presence of Bacteria [1]	BHM [2]	HSG or SG [3]	Fe Source
1	YES	YES	No HSG or SG	Dissolved Fe [4]
2	YES	YES	SG	Dissolved Fe [4]
3	YES	YES	HSG	Colloids [5]
4	NO	YES	HSG	Colloids [5]

[1] Either *Mycolicibacterium* sp. or *Pseudomonas* sp. [2] Modified Bushnell–Haas deprived of iron (see below). [3] Hybrid silica gel with CHA or LSC colloids (HSG) or silica gel deprived of colloids (SG). [4] Content of added dissolved Fe: 127 $\mu g \cdot L^{-1}$. [5] Maximum content of Fe: 84 ± 12 $\mu g \cdot L^{-1}$and 605 ± 79 $\mu g \cdot L^{-1}$ for CHA and LSC, respectively.

In order to assess the sole effect of pH variations on elemental solubilization, additional incubations in sterile BHM were performed under abiotic conditions over a fixed time (6 days) with the pH set using HNO_3 0.1 M.

The growth medium (BHM) was a modified Bushnell–Haas medium deprived of iron and composed of 22.5 $mg \cdot L^{-1}$ Na_2HPO_4-$2H_2O$, 20 $mg \cdot L^{-1}$ NaH_2PO_4-$2H_2O$, 20 $mg \cdot L^{-1}$ KCl, 100 $mg \cdot L^{-1}$ KNO_3, 65 $mg \cdot L^{-1}$ $(NH_4)_2SO_4$, 20 $mg \cdot L^{-1}$ $CaCl_2$-$2H_2O$ and 2 $g \cdot L^{-1}$ glucose. BHM was prepared with analytical reagents and UPW to maintain the iron

concentration at a low level. Prior to biotic incubations, bacteria were cultivated in a Luria–Bertani broth at 28 °C for 48 h, washed twice with sterile UPW water and the resulting cells were re-suspended to obtain an optical density (680 nm) of 0.04 corresponding to a cell concentration of 1–3 $\times$ 10^8 cells ml^{-1} in each of the three replicates.

Sampling was performed sacrificially in order to avoid any contamination. At each sampling time (1 h, 24 h, 3, 6 and/or 9 days), three wells of the microplate were sacrificed, and the sampled solution was immediately centrifuged (10,000$\times$ *g* for 10 min). Kinetic experiments (1 h to 9 days) under biotic conditions were performed in triplicates, while abiotic experiments, kinetics experiments and experiments as a function of pH at 6 days, were performed in duplicates.

2.4.3. Solution Analysis

The pH value was measured in clear supernatant after centrifugation at 10,000$\times$ *g* for 10 min using a pH micro-electrode (Orion^{TM} PerpHecT^{TM} ROSS^{TM}, Thermo Fisher Scientific, Waltham, MA, USA).

The optical density was measured prior to centrifugation using a spectrophotometer at 680 nm (OD_{680}) to assess the turbidity of the suspension related to the development of bacteria.

Analyses of released Fe, Mn, Cr, Pb and As concentrations were performed on centrifuged and acidified samples (2% *v*/*v*) with concentrated HNO_3 (Suprapur Merck, Darmstadt, Germany) samples, using an Inductively Coupled Plasma Mass Spectrometer (Agilent Technology 7700$\times$ ICP-MS, ^{45}Sc and ^{115}In internal standards, Santa Clara, CA, USA). The LOQ was 1 $\mu gFe \cdot L^{-1}$, 0.07 $\mu gMn \cdot L^{-1}$, 0.03 $\mu gCr \cdot L^{-1}$, 0.04 $\mu gPb \cdot L^{-1}$ and 0.04 $\mu gAs \cdot L^{-1}$.

The determination of carbohydrates was performed on centrifuged samples using a colorimetric method at 492 nm after a phenol (5% *w*/*w*)-sulfuric acid (95%) reaction [27]. Calibration was performed between 0 and 100 $mg \cdot L^{-1}$ using pure glucose solution (Rectapur Prolabo). Samples were diluted in UPW water before analysis.

The analysis of fluorescent organic compounds produced by bacteria was performed on a Shimadzu RF-5301 PC spectrofluorophotometer with a 150-W xenon lamp as the excitation source. Excitation emission matrix (EEM) spectra were obtained on centrifuged and diluted samples with 50 mM phosphate buffer (NaH_2PO_4-$2H_2O$, Na_2HPO_4-$2H_2O$) at a pH of 7.0 $\pm$ 0.1. The emission wavelength was scanned from 225 to 525 nm after excitation ranging from 220 to 450 nm at 5 nm increments. The analysis was conducted in a 1 cm quartz cell at 22 $\pm$ 1 °C. The fluorescence data were processed using the Panorama Fluorescence 3.1 software (LabCognition, Cologne, Germany). Fluorescence 3D analysis was performed only for experiments involving CHA colloids under both biotic (with *Pseudomonas* sp.) and abiotic conditions.

3. Results

3.1. Size and Chemical Composition of the Water-Mobilizable Submicrometric Fraction of Sediments

The size of the recovered colloids from both sediments (CHA and LSC) was relatively small, as 97 $\pm$ 2% (CHA) and 88 $\pm$ 1% (LSC) of the less than 1 µm size fraction was smaller than 450 nm. The fraction below 220 nm contributed to approximately 60% of the colloids. The colloids recovered from LSC sediments were enriched in the following size fractions: nano-colloids (<100 nm), the fraction between 450–700 nm and the fraction >700 nm, compared to the colloids recovered from CHA sediment (Figure 1). The mass of the recovered large colloids retained on the 0.2 µm filter (0.2–1 µm fraction) was found to be 2.7 $\pm$ 0.5 and 20.8 $\pm$ 1.0 mg/g_{DW} of the sediments for CHA and LSC, respectively.

The chemical composition of the total recovered fractions (<1 µm) and the fractions below 0.2 µm (small/nano-colloids and some potentially dissolved elements) is presented in Table 2.

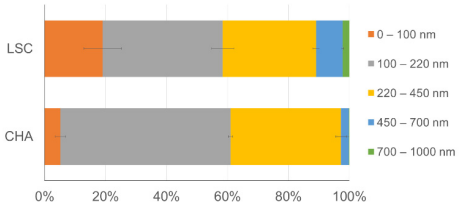

Figure 1. Size distribution by number of water-mobilizable colloids form Champsanglard (CHA) and L'Escourou (LSC) sediments. Error bars represent 1 SD calculated from triplicates.

Table 2. Chemical compositions (mg.L^{-1}) of the water-mobilizable submicrometric fractions recovered from the Champsanglard (CHA) and L'Escourou (LSC) sediments. The chemical composition (mg.L^{-1}) of the less than 0.2 µm and 0.2 to 1 µm sub-fractions are also presented.

Fraction	Al (mg·L^{-1})	Fe (mg·L^{-1})	Mn (mg·L^{-1})	Cr (µg·L^{-1})	As (µg·L^{-1})	Pb (µg·L^{-1})	C_{org} (mg·L^{-1})	N_{tot} (mg·L^{-1})	P_{tot} (mg·L^{-1})
CHA < 1 µm	3.20 ± 0.18	1.95 ± 0.28	0.26 ± 0.10	2.72 ± 0.20	3.3 ± 0.7	5.04 ± 1.05	4.09 ± 0.17	3.04 ± 1.26	0.29 ± 0.01
CHA < 0.2 µm	0.76 ± 0.12	0.60 ± 0.16	0.25 ± 0.12	0.8 ± 0.1	2.22 ± 0.32	0.95 ± 0.24	3.94 ± 0.47	3.21 ± 0.95	0.10 ± 0.01
CHA 0.2–1 µm	2.44 ± 0.16	1.34 ± 0.15	<LQ	1.91 ± 0.11	1.10 ± 0.53	4.08 ± 0.84	0.14 ± 0.31	<LQ	1.0 ± 0.1
LSC < 1 µm	27.16 ± 3.56	14.12 ± 1.84	0.09 ± 0.01	26.82 ± 3.36	8.55 ± 1.14	13.8 ± 1.73	12.35 ± 0.8	1.69 ± 0.31	5.20 ± 0.4
LSC < 0.2 µm	0.03 ± 0.11	0.06 ± 0.07	0.00 ± 0.00	0.17 ± 0.15	1.13 ± 0.05	0.07 ± 0.07	3.78 ± 0.80	0.91 ± 0.07	0.04 ± 0.01
LSC 0.2–1 µm	27.06 ± 3.54	14.06 ± 1.84	0.09 ± 0.01	26.64 ± 3.41	7.42 ± 1.16	13.73 ± 1.66	8.57 ± 1.14	0.78 ± 0.3	5.2 ± 0.4

LSC colloids present higher Al, Fe, Corg, Ptot and trace elements (Cr, Ni, As and Pb) content than CHA colloids. More than 97% of the released element in the <1 µm fraction were associated with large colloids (0.2–1 µm), except for Ntot, Corg and As, which were lower in large colloids, at 46, 69 and 87%, respectively. The molar ratio of Corg/Al (RAl) calculated for <0.2 µm fractions, indicates that LSC's <0.2 µm fraction was more organic (RAl = 50.6) compared to CHA's <0.2 µm fraction (RAl = 2.3). The same statement was conducted with RFe (Corg/Fe), equal to 14.2 for LSC and 1.4 for CHA. The RAl and RFe calculated for the 0.2–1 µm fraction showed a comparable RAl of 0.14 and 0.13 and an RFe of 0.03 and 0.02 for LSC and CHA, respectively. The <1 µm CHA fraction was enriched up to 3.8-fold in Mn and 1.8-fold in Ntot, compared to the <1 µm LSC fraction. The association of the elements to the large colloids was lower in comparison to LSC: 0.3%, 4.9%, 33% and 0% for Ntot, Corg, As and Mn, respectively, and from 45% to 80% for other elements.

3.2. Set-Up Validation

Results regarding the evolution of bacterial growth (OD_{680}) and pH for the four experimental conditions presented in Table 1 are reported in Figure 2 (note that only the results from experiments performed with *Mycolicibacterium* sp. and CHA colloids are presented here since similar trends were observed for LSC colloids and *Pseudomonas* sp.).

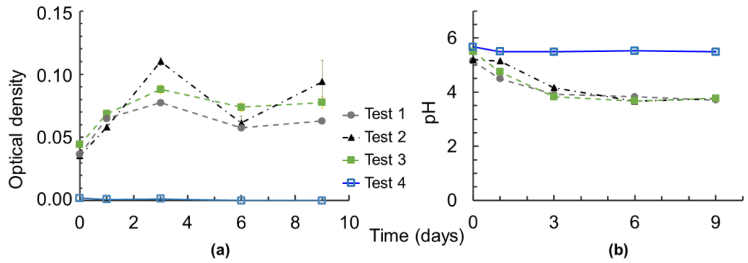

Figure 2. Evolution of (**a**) the optical density measured at 680 nm and (**b**) the pH for the four conditions presented in Table 1. The incubation of bacteria in BHM * spiked with dissolved Fe (Test 1); bacteria and silica gels in BHM spiked with dissolved Fe (Test 2); bacteria with silica gel-containing CHA colloids in BHM (Test 3); and silica gel containing CHA-colloids under abiotic conditions in BHM (Test 4). Results are reported here only for *Mycolicibacterium* sp. and Champsanglard colloids for the purpose of clarity. Error bars represent 1 SD. * BHM-modified Bushnell–Haas growth medium, depleted with dissolved iron.

Under abiotic conditions (i.e., control case, Test 4), the optical density remained negligible (<0.003, Figure 2a) and the pH showed no significant changes (at 5.7 ± 0.1, Figure 2b) throughout the incubations. Bacterial growth was evidenced in all biotic experiments (Tests 1, 2 and 3) by a regular increase in OD_{680} over the first 3 days (from about 0.04 up to 0.12), followed by a plateau or a slight decrease (Figure 2a). Bacterial growth was accompanied by a decrease in pH from 5.3 to 3.7 during the first 3 days and remained constant until the end of incubation. Experiments conducted with bacteria in BHM medium spiked with dissolved Fe and without silica gel (Test 1), and always showed the lowest OD_{680} values. OD_{680} values from biotic experiments performed either with SG (silica gel without colloids) and growth medium spiked with dissolved Fe (Test 2) or with HSG (colloids embedded in silica gel) in growth media depleted with dissolved Fe (Test 3) show similar values (it remains of the same order of magnitude, even if the behavior for test 2 with *Mycolicibacterium* sp. was quite erratic between 3, 6 and 9 days) and no general tendency pointing towards a higher growth, regardless of the conditions.

3.3. Microbial Solubilization of Sedimentary Colloids with Time

3.3.1. Bacterial Growth

Figure 3 shows the results from the regular monitoring (1 h to 9 days) of the optical density and pH for all experiments performed with further measurements of dissolved metal(loid) concentrations (Table 1, Tests 3 and 4), i.e., experiments performed with colloids extracted from CHA and LSC sediment in Fe-restricted BHM medium under abiotic (CHA abiotic, LSC abiotic) and biotic conditions using *Mycolicibacterium* sp. and *Pseudomonas* sp.

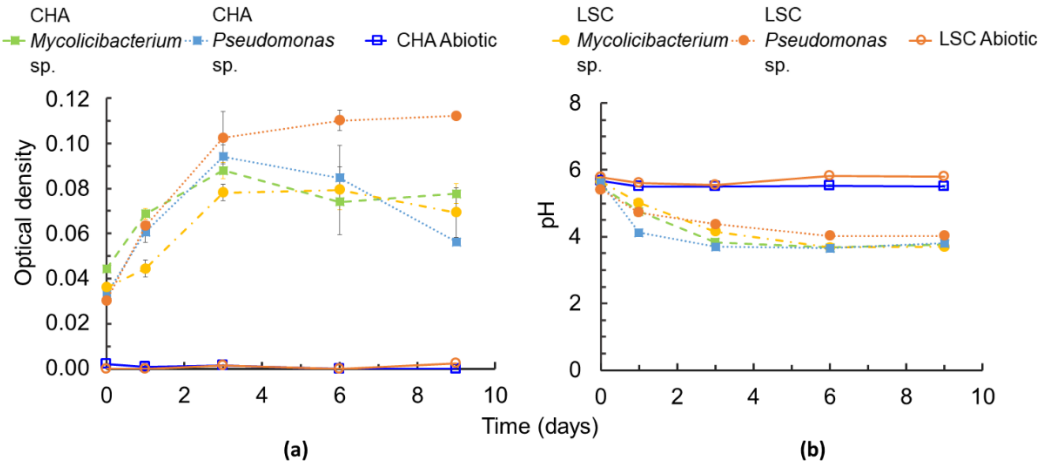

Figure 3. Evolution of (**a**) the optical density measured at 680 nm and (**b**) the pH for all experiments used to study iron bioavailability from sedimentary colloids under biotic (*Mycolicibacterium* sp. and *Pseudomonas* sp.) and abiotic conditions as a function of time. Experiments performed with two sedimentary colloids. CHA = Champsanglard and LSC = L'Escourou colloids. Error bars represent 1 SD.

Variations in the optical density and pH in biotic experiments with sedimentary colloids under restricted dissolved Fe conditions showed a similar evolution, with a regular increase in OD_{680} over the first 3 days of the experiment (from 0.037 ± 0.007 to 0.09 ± 0.01, Figure 3a), and a decrease in the pH, from 5.6 ± 0.2 down to 4.0 ± 0.3, after 3 days of the experiment (Figure 3b). After 3 days of incubation, similar tends were observed for the experiments performed with both strains with CHA-colloids and *Mycolicibacterium* sp. with LSC colloids, with a slight decrease in OD_{680} between 3 and 9 days (down to 0.067 ± 0.011), and a stabilization of pH at 3.75 ± 0.05. The evolution of OD_{680} and pH for the experiment performed with *Pseudomonas* sp. with LSC-colloids was a bit different, with a plateau observed for OD_{680} instead of a slight decrease (from 0.10 ± 0.01 at 3 days to 0.11 ± 0.01 at 9 days) and a final pH value higher of 0.15 pH unit in average (4.0 ± 0.1). The

total glucose amount in the solution was measured at the end of the experiment to verify that the carbon source was not limiting. In all experiments, more than 75% of the initial amount of carbohydrates was still present after 9 days of experiments (Supplementary Materials Figure S2).

The bacterial growth was accompanied by the release of organic compounds in the solution. A solution from the control experiment without colloids (only silica gel, Test 2) in the presence of *Pseudomonas* sp. was used to assess the contribution of the sole bacteria. The fluorescence of the produced organic compound (EEM results) is reported in Figure 4.

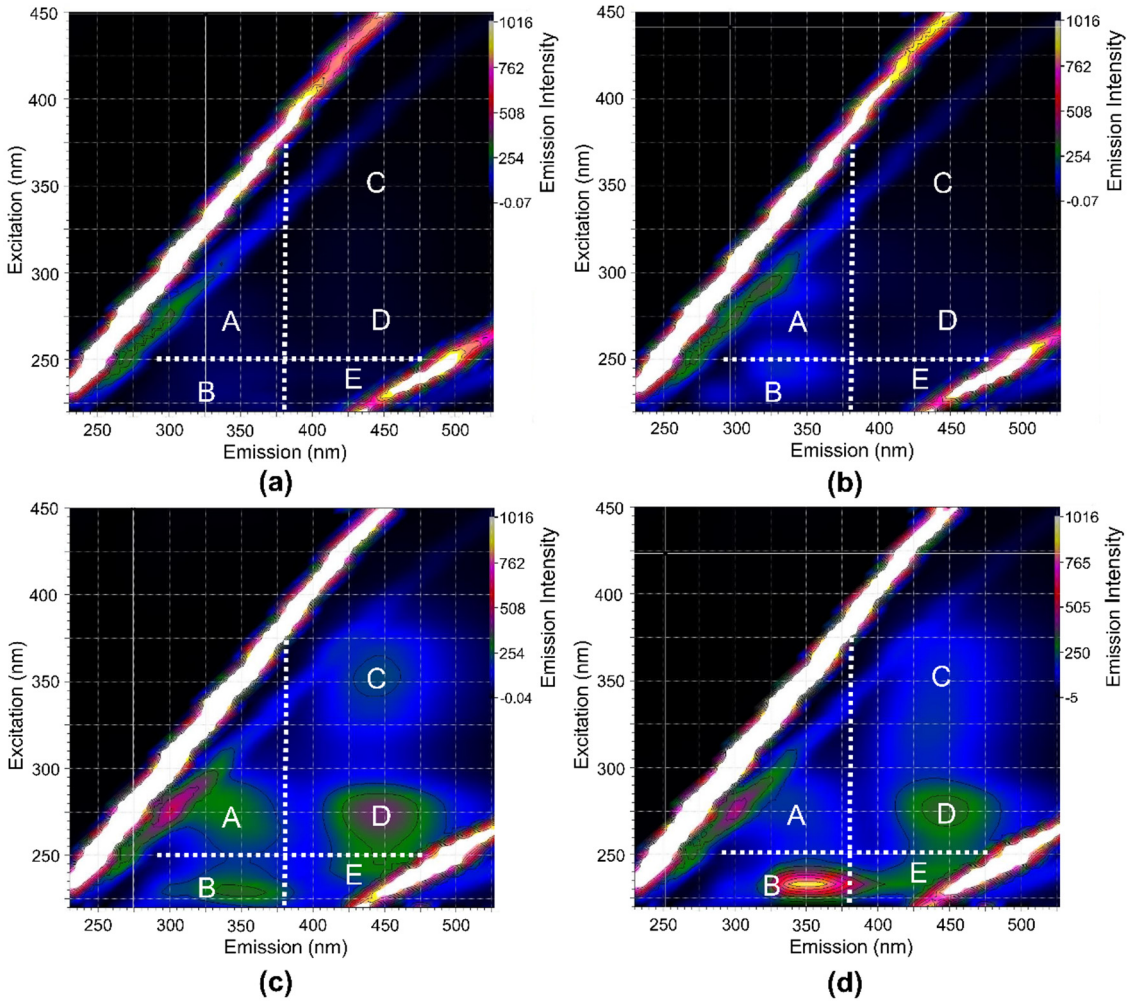

Figure 4. Fluorescence excitation–emission matrix of solutions for the following experiments: (**a**) 1 h CHA colloids under abiotic conditions; (**b**) 9-day CHA colloids under abiotic conditions; (**c**) 9-day CHA colloids with *Pseudomonas* sp.; (**d**) 9-day silica gel with *Pseudomonas* sp.

The starting solution did not display any significant signal, except for the contribution of water (Figure 4a). Five main peaks (named A, B, C, D and E; see Figure 4c,d) were observed at a similar excitation/emission position in the matrices, but with different intensities, under both of the tested biotic conditions (with or without colloids) after 9 days. Note that peak intensities are not necessarily due to the variation in the quantity of the reactive compounds but may vary due to a combination of factors such as the overlap of signals from different compounds, or the possible decrease in the fluorescence due to extinction after binding with metallic elements (quenching). According to the literature, peaks A (region IV from [28]) and B (region II) can be attributed to proteins/tryptophan-like molecules and in general microbial soluble by-products [29]. Peak C (region V) is usually associated with humic-like substances, whereas peak E (region III) is usually attributed to

fulvic-like substances. Peak D (region III) can be related either to humic- and fulvic-like substances. A slight contribution in the region of peaks A and B was observed in the abiotic experiments after 9 days (Figure 4b). As no growth was observed from OD_{680} measurements and no acidification was observed under abiotic conditions, we can expect this organic matter to originate from the organic compounds embedded in silica gel rather than bacterial activity during the experiment.

3.3.2. Iron Release in the Solution as a Function of Time

Under abiotic conditions, the release of Fe was stable throughout the complete duration of the experiments, and with similar values for both colloids studied (4 ± 2.5 $\mu g \cdot L^{-1}$ on average over the whole experiment). Then, in the presence of bacterial strains and colloids, a progressive increase in Fe aqueous concentrations was observed starting at 3 days and until the end of the experiments (9 days). After 9 days, iron concentrations were higher under biotic conditions than they were under abiotic conditions, by a 4 to 5-fold factor for experiments with *Pseudomonas* sp., and 6- to 10-fold factor with *Mycolicibacterium* sp. (Figure 5b).

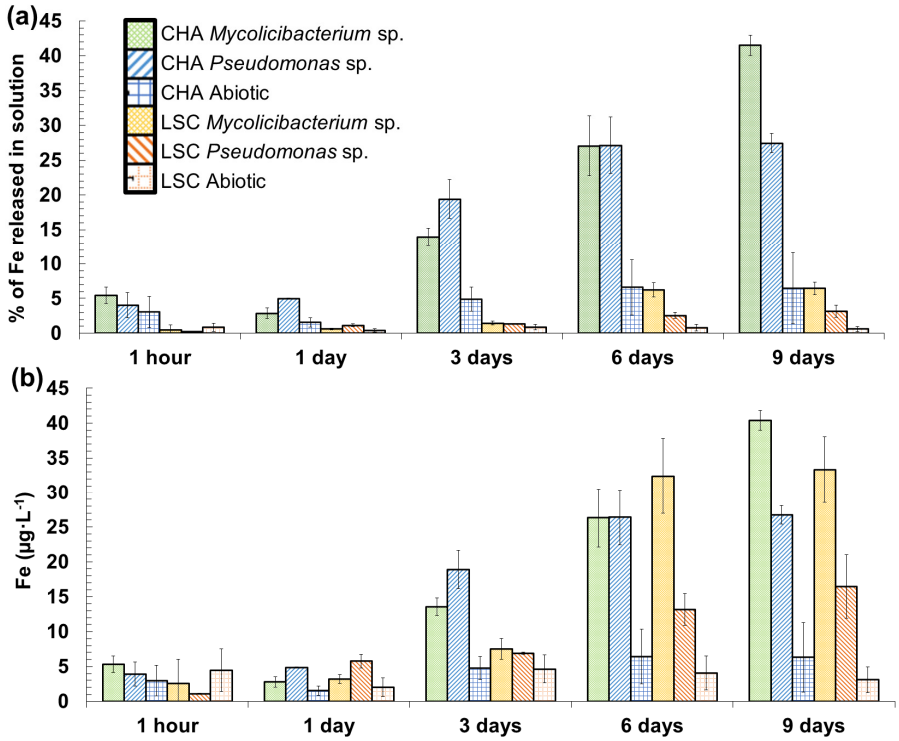

Figure 5. Evolution as a function of time in iron released from sedimentary colloids under both biotic (either with *Mycolicibacterium* sp. or *Pseudomonas* sp.) and abiotic (no pH buffer) conditions for the two Champsanglard (CHA) and L'Escourou (LSC) colloids: (**a**) percentage of released iron relative to the total Fe content of the colloid; (**b**) concentration of Fe in solution ($\mu g \cdot L^{-1}$). Error bars represent 1 SD.

Comparing the effect of the colloid nature, the iron concentration in the solution is 20% to 50% higher after 9 days in the case of CHA colloids (40.4 ± 1.4 and 26.7 ± 1.4 $\mu g \cdot L^{-1}$ in the presence of *Mycolicibacterium* sp. and *Pseudomonas* sp., respectively) than with LSC colloids (33.3 ± 4.7 and 16.5 ± 4.6 $\mu g \cdot L^{-1}$ in the presence of *Mycolicibacterium* sp. and *Pseudomonas* sp., respectively). Additionally, after 9 days, *Mycolicibacterium* sp. seemed to be more efficient at extracting iron from colloids than *Pseudomonas* sp., with aqueous concentrations that were 50 to 90 % higher for CHA colloids and LSC colloids, respectively (Figure 5a).

Note that even after 1 h of incubation, a significant amount of Fe was measured in the solution (up to 3.4 $\mu g \cdot L^{-1}$ after 1 h, see Figure 5b), even under abiotic conditions. Such an effect results from the fast equilibrium between the growth medium and the solution from HSG porosity. Note that HSG is a highly porous gel, and the pore solution may already be enriched in iron before the start of incubation as some new solid-solution equilibria may be attained after the HSG sterilization. Up to 34% $\pm$ 7 and 6.5% $\pm$ 0.08 of total Fe was released to the solution from CHA and LSC colloids, respectively, after 9 days of incubation (Figure 5a).

3.3.3. Trace Elements Released in the Solution as a Function of Time: Mn, Pb, Cr and As

Along with iron solubilization, other elements (Mn, Pb, Cr and As, see Figure 6) were released into the solution.

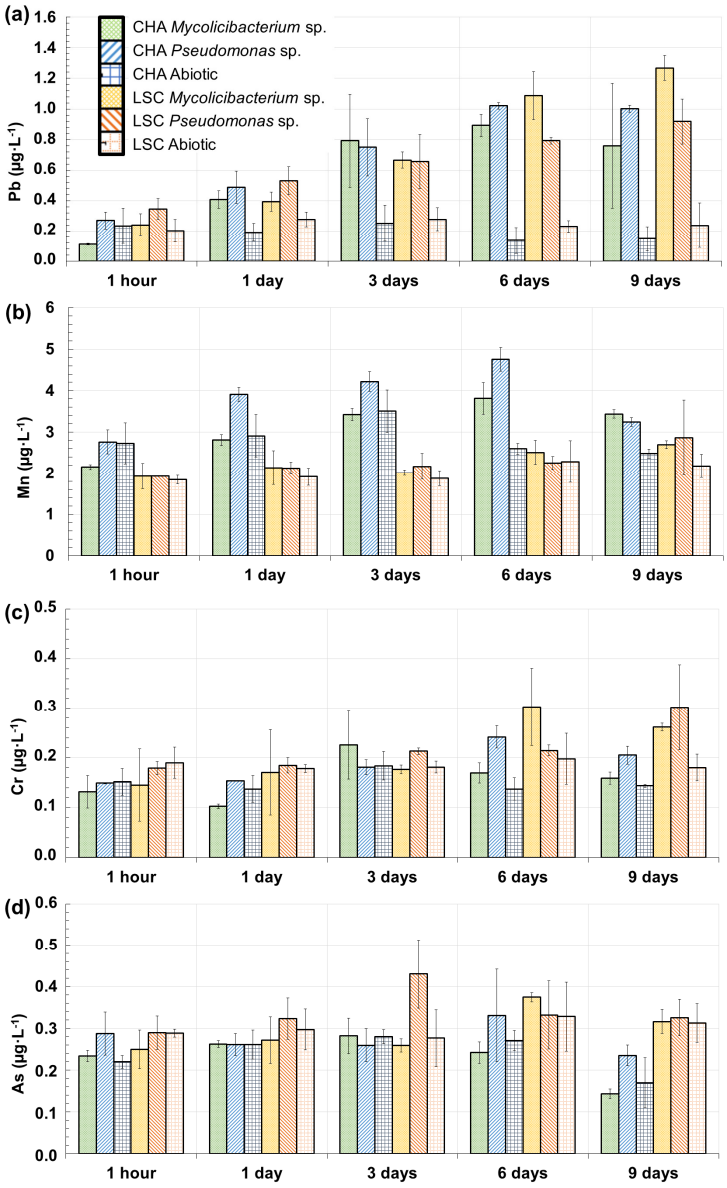

Figure 6. Evolution as a function of time for (**a**) lead (Pb), (**b**) manganese (Mn), (**c**) chromium (Cr) and (**d**) arsenic (As) concentrations ($\mu g \cdot L^{-1}$) in the solution for experiments performed with sedimentary colloids under biotic (either with *Mycolicibacterium* sp. or *Pseudomonas* sp.) and abiotic conditions and for the two Champsanglard (CHA) and L'Escourou (LSC) colloids. Error bars represent 1 SD.

As for lead, the Pb concentrations in the solution follow roughly the same trend as iron, with stable values throughout the duration of the experiments under abiotic conditions and with similar values for both the tested colloids (0.14 ± 0.06 $\mu g \cdot L^{-1}$ on average over the whole experiment) (Figure 6a). In addition, the concentrations in the solution increased in a similar way in the presence of both bacterial strains for both colloids starting at day 1. After 9 days, Pb concentrations were higher under biotic conditions than under abiotic conditions by a 5- to 9-fold factor for experiments with *Pseudomonas* sp., and an 8-fold factor with *Mycolicibacterium* sp. Comparing both colloids, the release of lead after 9 days of incubation was comparable in the case of CHA colloids with both strains (0.76 ± 0.41 and 0.89 ± 0.02 $\mu g \cdot L^{-1}$ in the presence of *Mycolicibacterium* sp. and *Pseudomonas* sp., respectively) and for LSC colloids with the presence of *Pseudomonas* sp. (0.81 ± 0.15 $\mu g \cdot L^{-1}$), while the values were slightly higher for the incubation of LSC colloids with *Mycolicibacterium* sp. (1.16 ± 0.04 $\mu g \cdot L^{-1}$, +40% on average compared to the other conditions).

Regarding manganese, two different behaviors in the solution were observed, depending on the tested colloids. First, in the experiment performed with LSC colloids, a stable Mn concentration over 9 days was measured (fluctuating between 1.84 and 2.86 $\mu g \cdot L^{-1}$) (Figure 6b) under both biotic and abiotic conditions, so the bacteria did not have a significant effect on the release of Mn. Then, for experiments performed with CHA colloids, an increase in the concentration under biotic conditions from 2.46 ± 0.30 $\mu g \cdot L^{-1}$ at 1 h to 4.28 ± 0.47 $\mu g \cdot L^{-1}$ at 6 days was observed followed by a decrease to 3.34 ± 0.09 $\mu g \cdot L^{-1}$ at 9 days. Under abiotic conditions, the increase was from 2.73 to 3.50 $\mu g \cdot L^{-1}$, from 1 h to 3 days, before decreasing to 2.48 $\mu g \cdot L^{-1}$ at 9 days. Therefore, a biotic effect was observed only for CHA colloids, with an increase in aqueous concentrations of 60% and 20% after 6 and 9 days of the experiment, respectively.

As for chromium, the concentration over 6 days fluctuated between 10 and 30 $\mu g \cdot L^{-1}$ (Figure 6c) under both biotic and abiotic conditions and for both colloids, so no significant effect of bacteria was observed. At 9 days, higher Cr concentrations in the solution were observed for experiments performed with *Pseudomonas* sp. with CHA colloids (0.20 ± 0.02 $\mu g \cdot L^{-1}$) and LSC colloids (0.30 ± 0.09 $\mu g \cdot L^{-1}$), than under abiotic conditions (0.16 ± 0.02 on average for both colloids).

Regarding arsenic, there was a stable concentration over 9 days (0.28 ± 0.1 $\mu g \cdot L^{-1}$) (Figure 6d) under both biotic and abiotic conditions and for both colloids, so no significant effect of bacteria was observed.

To summarize, there was a significant biotic effect on the dynamic of Pb released into the solution for both tested colloids after 1 day (Figure 6a), and there was also a significant effect on Cr after 6 (CHA colloids) or 9 days (LSC colloids) (Figure 6c). There was a biotic effect only for CHA colloids for Mn (Figure 6b) and no significant biotic effect on As (Figure 6d). In addition, the colloids' origin did not have a significant effect on the overall dynamic of release Pb's into the solution. Some differences start to appear during the 9-day experiments for Cr and As, and there is an exception for Mn with significant differences in aqueous concentrations between experiments performed with the two colloids after only one day.

3.4. Release of Fe, Mn, Pb, Cr and As into the Solution from the Colloids as a Function of pH

Since the release of elements occurred at different pH conditions under abiotic and biotic conditions (biotic incubations showed an acidification of the growth medium by about 2 pH units) (Figures 2b and 3b), additional abiotic incubations were performed to evaluate the role of the pH on metal(loid)s' release from colloids. Additional abiotic incubations were performed at the imposed pH and content of solubilized elements compared to biotic incubations (described previously in Sections 3.3.2 and 3.3.3). Fe, Mn, Pb, Cr and As concentrations are reported in Figure 7 as functions of pH.

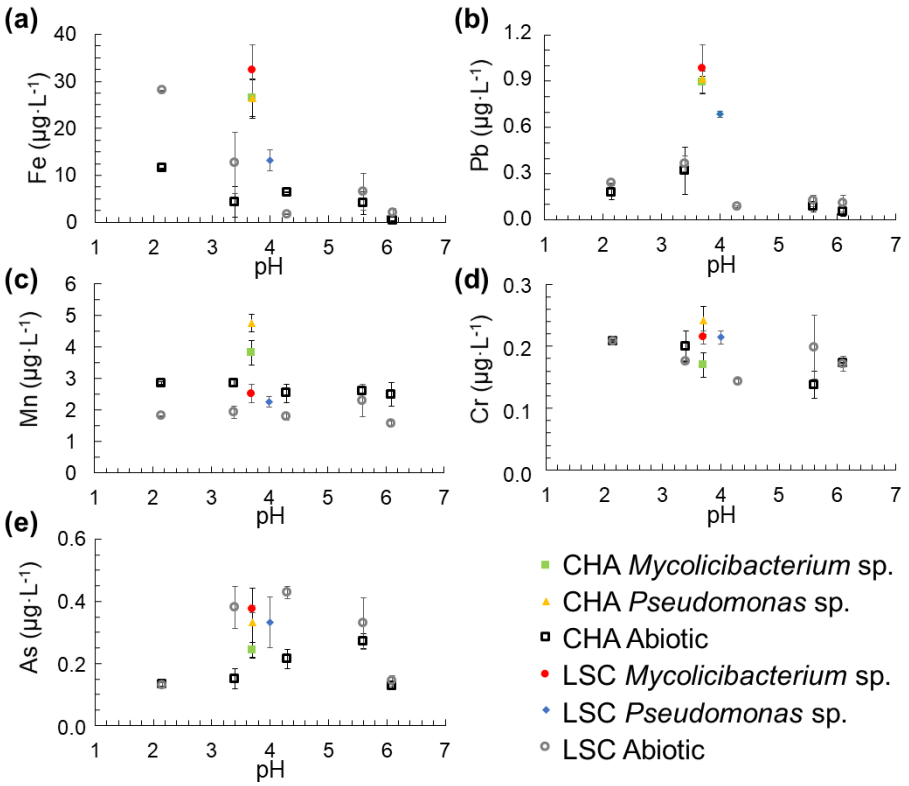

Figure 7. Aqueous concentrations of (**a**) iron (Fe), (**b**) lead (Pb), (**c**) manganese (Mn), (**d**) chromium (Cr) and (**e**) arsenic (As) as a function of pH after 6 days for fixed pH experiments without bacteria (empty symbols) for both CHA and LSC colloids. Results from biotic incubations at 6 days are also reported (full symbols). Error bars represent 1 SD.

Aqueous concentrations in abiotic conditions show (i) no significant differences between the two colloids studied (Figure 7b–e), except for Fe at a pH of 2.1 with concentration 3 times higher for LSC colloids than for CHA colloids, at 28.1 and 11.5 $\mu g \cdot L^{-1}$, respectively (Figure 7a); and (ii) no significant evolution of As, Cr and Mn concentrations with decreasing pH values (Figure 7c–e), and increasing Pb (from 0.08 $\mu g \cdot L^{-1}$ to 0.21 $\mu g \cdot L^{-1}$ on average, Figure 7b) and Fe concentrations (from 2.0 $\mu g \cdot L^{-1}$ to 28.1 $\mu g \cdot L^{-1}$ and from <1 $\mu g \cdot L^{-1}$ to 11.5 $\mu g \cdot L^{-1}$ for LSC colloids and CHA colloids, respectively, Figure 7a) with decreasing pH values (from pH 6.1 to 2.1).

Comparisons between concentrations measured under biotic and abiotic conditions show different behavior depending on the element and the colloids tested. Aqueous As and Cr concentrations under biotic conditions (0.32 ± 0.08 $\mu g \cdot L^{-1}$ and 0.21 ± 0.04 $\mu g \cdot L^{-1}$ for As and Cr, respectively) are in the same range of values as abiotic conditions (0.20 ± 0.13 $\mu g \cdot L^{-1}$ and 0.18 ± 0.05 $\mu g \cdot L^{-1}$ for As and Cr, respectively) (Figure 7d,e). The presence of bacteria induces an increase in aqueous Mn concentrations under biotic conditions compared to abiotic conditions but only for CHA colloids, by up to a 1.7-fold factor (4.75 ± 0.29 $\mu g \cdot L^{-1}$ for CHA-colloids and *Pseudomonas* sp. and 2.37 ± 0.8 $\mu g \cdot L^{-1}$ on average under abiotic conditions) (Figure 7c). There was a significant biotic effect on Fe and Pb concentrations regardless of the colloids used, with an increase in aqueous concentrations under biotic conditions (pH = 3.7) compared to abiotic conditions (pH = 3.4), with up to a 6- and 4-fold factor for Pb and Fe, respectively (Figure 7a,b). Note that in the case of a significant biotic effect on the increase in aqueous concentrations (Fe and Pb with both colloids and Mn with CHA-colloids), aqueous concentrations may reach higher values than under abiotic conditions, with H^+ concentrations that are 40 times higher (pH values from 3.7 to 2.1).

4. Discussions

4.1. Quality of the Submicrometric Fraction Recovered from Bottom Sediments

As expected, bottom sediments collected from two dam reservoirs implemented in contrasting geological contexts (crystalline substratum for CHA and calcareous for LSC) differed in chemical composition and grain size distribution (Tables S1 and S2). Both sediments were fine-grained but the D50 was different and corresponded to a grain size of 17.7 µm (CHA) and 6.5 µm (LSC). The content in the clay fraction in CHA and LSC sediment was relatively low (1.2% and 9.8%, respectively) compared to natural lakes and was probably related to the specific hydrodynamics of dam reservoirs, which are more river-like than lacustrine. The distribution of fine particles on the bottom depends largely on the flow velocity [30]. A higher abundance of fine particles occurs mainly in areas where the water residence time is long (lakes, not dammed reservoirs). The sediments deposited in the areas immediately downstream of the dam or in the upper part of the reservoir system contain a coarser texture [31,32]. Aside from a relatively low content of clay fraction, both sediments were capable of releasing colloids (operationally defined as particles within the size range from 1 nm to 1 µm in at least one dimension) [33] upon sediment resuspension. The higher potential of LSC sediment for releasing large colloids compared to the CHA sediment is probably related to the higher clay fraction content and/or higher pH value of the LSC sediment compared to the CHA sediment (7.5 for LSC and 6.5 for CHA). The pH of the sediment, together with colloid composition, ionic strength and dissolved organic matter content, determines the surface charge of the colloids, and surface charge, along with colloid size and hydrophobicity, affects colloid dispersibility. Alkaline conditions increase the negative surface charge of both the colloid and sediment matrix, and thus reduce interparticle attraction and promote the stronger repulsion of colloids by the negatively charged solid matrix [34–36]. Thus, higher colloids amount released from LSC sediment can also be explained by weaker colloids association with the sediment matrix related to alkaline conditions. It was also observed that the released colloids differed in terms of the relative size distribution. A higher release of nano-colloids by LSC sediment (Figure 1) may be explained by the more organic character of <0.2 µm fraction and thus enhances organic colloids' repulsion from mineral surfaces, while the R_{Al} (C_{org}/Al) and R_{Fe} (C_{org}/Al) calculated for the 0.2–1 µm fraction indicate a more mineral composition, with comparable values for LSC and CHA, respectively (see Section 3.1 in Results). The higher content of larger colloids (Figure 1) released by LSC sediments (calcareous character) can be explained by the enhanced formation of organo-mineral associations in the presence of Ca^{2+} and Mg^{2+}, which facilitate cation bridging and thus the aggregation of small colloids to large-sized colloids [37]. Since the concentration of large colloids released from LSC sediments was 12 time higher than that from CHA sediments, it is possible that a higher number of particles per unit volume increased particle collision and allowed its aggregation [38].

The measurement of colloid size distribution (measurement by number, Figure 1) indicated that mobilized colloids were relatively small; up to 97 ± 2% (CHA) and 88 ± 1% (LSC) of colloids were lower than 450 nm, with the fraction below 220 nm, approximatively representing 60%. The chemical composition of large colloids (0.22–1 µm fraction) and the fraction below 0.22 µm (containing small/nano-colloids and truly dissolved elements if any) was significantly different (Table 2). For the LSC sample, 99.9% of Al, 99.6% of Fe, 99.5% of Pb, 99.3% P, 98.8% of Mn and 99.4% of Cr released in the fraction below 1 µm, was found in large colloids. These percentages were lower for As (86.8%), C_{org}. (69.4%) and N_{tot}. (46.1%). For CHA, 81.1% of Pb, 76.1% of Al, 70.3% of Cr, 69% of Fe and 67.2% of P released in the fraction below 1 µm, was found in large colloids. These percentages were much lower for As (33.1%) and C_{org}. (3.5%). Large CHA colloids contained negligible amounts of Mn and N_{tot} (values below the detection limit, see Table 2). As shown in Supplementary Materials Table S3 and deduced as the mass of released elements over the mass of large colloids, the nature of large colloids recovered from CHA and LSC sediments contained a similar range in the concentration of Al, Fe and Cr, despite their higher content in CHA sediment. The large colloids released from CHA sediments were enriched in Pb and As,

compared to large LSC colloids, which was in concordance with the chemical composition of CHA sediments. However, the large LSC colloids were enriched in P and C, whereas the content of P was higher in CHA sediment. These observations demonstrate the various affinities of elements for the smaller and larger submicrometric fractions of sediments and that this repartition depends on sediment quality.

Our finding indicates that surface sediment deposited in the bottom of LSC and CHA reservoirs have a strong potential to release nutrients (e.g., P, N) and potentially toxic elements (e.g., Pb, As) to water upon resuspension. The mobilized elements were mainly associated with large colloidal fractions (0.2–1 µm). The large colloids recovered from CHA and LSC sediments were found to contain 3.6% and 18% of the total sedimentary P, 2.3% and 2.7% of the total sedimentary Al, 1.2% and 1.3% of the total sedimentary Fe, 1.2% and 2.1% of the total sedimentary Cr, 2.7% and 2.1% of the total sedimentary Pb, and 1.1% and 1.2% of the total sedimentary As, respectively. This highlights the importance of this fraction in the mobility of nutrients and contaminants at the sediment/water interface. Our results indicate that the fractions below 0.2 µm (operationally considered as dissolved in many environmental studies) contain colloids and nano-colloids (<100 nm). This highlights that the studied sediments contain a highly mobile colloidal fraction that may be a significant contributor to the potential mobilization of nutrients and metallic elements from sediments to the water column.

4.2. Encapsulation of Sedimentary Colloids in Porous Silica Gel

If HSG is allowed to separate bacteria from purified and size-calibrated clay minerals in order to deeply study the biochemical interactions at the colloidal particle–bacteria interface [23,39,40], we showed the feasibility of using such a methodology to study the ability of bacteria to sequester nutrients from sedimentary colloids that are heterogenous in size and chemical composition (Figure 1 and Table 2).

This feasibility was confirmed by the following findings:

(a) No microbial growth and no acidification of the growth media were observed under "abiotic" conditions (Test 4, Table 1 and Figure 2), reflecting the assured sterility of the bioassay during incubation. The sterility had to be checked, as recovered sedimentary colloids (fraction <1 µm) may have contained indigenous microorganisms that settled with the sediments in the aquatic system. It has been reported that the concentration of bacteria in bottom sediments can be 10–1000 times higher than in the overlying water, and that bacterial activity and abundance are generally highest in the surface sediment and decrease with sediment depth [41–44]. Since surface sediments were collected for colloid extraction and bacteria tend to attach to smaller particles because a larger surface area provides them with more attachment sites [45–47], inaccurate sterilization may therefore impair the effect of the tested bacteria by the action of the bacteria recovered during colloid extraction.

(b) The silica gels were confirmed to be biocompatible. Silica gels were synthesized by acid-catalyzed hydrolysis and base catalyzed condensation processes of tetraethyl orthosilicate in a closed system, which involves the release of ethanol, which can be toxic for bacteria. The presence of such residue (if any) after rinsing had to be checked. However, the greater bacterial growth in the presence of SG and HSG rather than with no solid (comparison of Tests 2 and 3 with Test 1), suggests a nontoxicity of the gels, and even a promoting effect of the presence of solid surfaces, such as silica gels in this case.

(c) There was no negative effect of the presence of colloids embedded in silica gels was observed on the bacterial growth (comparison of Test 2 with Test 3, Table 1), so no toxicity effect of metal(loid)s appeared at this level and time of exposure. This has to be checked, as the tested colloids contained potentially toxic elements such as Pb and As (Table 2, Figure 6).

(d) No negative effect on bacterial growth was measured under restricted dissolved Fe conditions in the presence of HSG (comparison of Test 2 with Test 3, Table 1), indicating that bacteria can manage their growth using elements coming from sedimentary colloids.
(e) There was no spontaneous release of elements from colloids embedded in silica gel. Silica gel is considered to be chemically and mechanically inert and non-degradable by the microorganisms [48]. The use of a sol-gel process allows for the creation of a mineral hybrid material whose porosity depends on the synthesis parameters. In our study, TEOS hydrolysis was obtained at highly acidic conditions (pH < 2) and through polymerization by increasing the pH to about 5. We did not assess the pore's size and its connectivity, but no spontaneous release of elements from the three-dimensional silica network was observed under abiotic conditions (Test 4, Table 1 and Figure 2). Since encapsulated suspensions consisted of fractions 0.2–1 µm (large colloids) and <0.2 m (small colloids and dissolved) in size, the lack of the spontaneous release of elements from the silica matrix suggests that the silica gels used had a pore size that did not allow colloids to be released from them, and that the dissolved fractions (if there were any) was washed out during the gel synthesis procedure.
(f) Note that due to the diffusion through the gel, equilibration with the solution may not be instantaneous and this may have an impact on the kinetics of the elements released to the solution. However, the equilibration appeared relatively fast, within an hour, as indicated by the stable pH and elemental concentrations under abiotic conditions (Figures 2 and 6).

4.3. Bioavailability of Colloidal Iron for Bacteria

Iron is an essential nutrient for living organisms. Since iron is quite insoluble under aerobic conditions and circumneutral pH, some bacteria are able (to assure their metabolic activity) to accelerate mineral dissolution directly through the acquisition of limiting nutrients from minerals or indirectly through the release of metabolic by-products that lower the solution's pH, complex dissolved elements, and/or change mineral saturation states [47,49]. As shown in Figures 3 and 4, both tested bacteria *Pseudomonas* sp. and *Mycolicibacterium* sp. were able to assure their microbial activity in the presence of colloids as a sole source of iron. As shown in Figure 2, similar patterns were observed for optical density and pH the after inoculation of the growth medium spiked with dissolved Fe (Test 1) and in the growth medium depleted with dissolved iron, which contained sedimentary colloids as a sole source of Fe (Test 3). In the natural environment under aerobic conditions, Fe is commonly present in the form of Fe(oxy)hydroxides or is associated with organic compounds. Numerous studies have shown that bacteria employ various strategies to acquire mineral nutrients such as acidification, the synthesis of siderophores and organic acids, or the colonization of mineral surfaces [50–53]. As expected, nutrient uptake by bacteria involved the release of Fe into the solution, demonstrating the implication of microbial metabolites in the solubilization of colloidal Fe phases. The observed Fe mobilization could be related to the acidification of the growth medium, from 6 down to 3.7 (Figure 3), and the complexation process. Indeed, the incubations performed at a fixed pH indicated that Fe release under similar pH conditions was increased by up to a seven-fold factor in the presence of bacteria compared to abiotic conditions (Figure 7). For most of the conditions tested, the Fe released in the presence of bacteria (pH = 3.7) was even higher than at a pH of 2 under abiotic incubations. Such a solubilization effect may be due to the exudation of soluble iron chelating agents on top of the acidification. Such a high capability to form complexes with Fe was documented in particular for multi-dentate acids and siderophores [54], molecules that can be produced by the bacteria used in this study. *Pseudomonas* sp., for instance, is known to have an effect on the release of iron from solid phases even when not in direct contact with the solid surface [55] as in our case with HSG.

There is strong evidence that *Pseudomonas* sp. and *Mycolicibacterium* sp. did not have the same potential to release Fe from colloids. As can be seen in Figure 5, the presence of bacteria increased Fe mobilization. After 3 days of incubation, the release of Fe was faster

from CHA compared to LSC colloids, and for both bacteria tested. This faster release could be associated with the quality of colloids and Fe speciation. The submicrometric fraction recovered from LSC sediments was 7 times richer in Fe compared to CHA, and 99.3% of the Fe was associated with large colloids (fraction between 0.2 and 1 µm). The total amount of Fe recovered from the CHA sediment (in the fraction below 1 µm) was 7 times lower compared to the amount extracted from the LSC sediment (Table 2). However, surprisingly, a greater release of Fe from CHA colloids was observed after 3 days of incubation and for both bacteria tested. This may be related to the higher content of small Fe colloids (fraction below <0.2 µm) in the CHA colloids. Clearly, at the beginning of the incubation, the microorganisms responded to the smaller, more available fraction. This is consistent with the studies of Gottselig et al., 2017 and Saeed et al., 2018 [12,56], who reported that for P, nano and small colloids (<0.45 µm) significantly affect its bioavailability and facilitate the transport of P. At the end of incubation, the release of Fe from CHA colloids was higher in the presence of *Pseudomonas* sp. This bacterium solubilized 27% of the total Fe (fraction <1 µm) and 80% of the iron associated with small colloids (fraction <0.2 µm). For the LSC colloids, the amount of mobilized Fe was 10 times greater compared to the amount of Fe associated with small colloids. These results indicate that in the case of LSC, the released Fe mainly originated from large colloids, and it demonstrates that large colloids are also bioavailable for the two tested bacteria. As shown in Figure 5, the potential of *Mycolicibacterium* sp. to release Fe from colloids was higher compared to *Pseudomonas* sp. Unfortunately, it is nearly impossible to determine the relative contribution of large and small colloids to the total budget of the released iron.

Our results demonstrate that (i) the principal fraction carrying Fe was large colloids (99% and 71% of the total Fe recovered in submicrometric fractions from LSC and CHA sediments, respectively); (ii) small and large Fe colloids are bioavailable for *Mycolicibacterium* sp. and *Pseudomonas* sp. under the tested conditions; (iii) a higher amount of Fe in LSC colloids compared to CHA did not result in a higher Fe concentration in the solution, yet the growth curves for the two tested bacteria were comparable; (iv) differences in the composition of colloids had no apparent effect on microbial growth; and (v) the potential of *Mycolicibacterium* sp. to release Fe from colloids was higher compared to *Pseudomonas* sp. under the tested conditions.

4.4. Solubilization of Colloids and the Impact on the Release of Pb, Mn, Cr and As

It is generally accepted that sediments act as a source and sink of nutrients and pollutants, which accumulate in lakes and reservoirs and tend to be released into overlying waters as a result of changes in the physio-chemical properties of the sediments or water.

Water mobilizable colloids recovered from CHA and LSC sediments carried potentially toxic elements such as Pb, Cr and As. Up to 99.5% (LSC) and 81% (CHA) of the total colloidal Pb was associated with large colloids (fraction 0.2–1 µm). Large colloids were also the principal bearing phases for Cr (99% and 70% for LSC and CHA, respectively) and As (87% and 33% for LSC and CHA, respectively).

Here, the (bio-)dissolution of colloids was also accompanied by the release of potentially toxic elements (trace metal(loid)s). In particular, Pb was released into the solution in high quantities in the presence of bacteria compared to abiotic conditions (increased by more than a 3-fold factor). Similarly, for Fe, the complexation with dissolved organic compounds may explain part of this behavior. Indeed, protein-like soluble bacterial product with fluorophores were evidenced here (Figure 5) and have been documented as being able to sequester Pb [57].

The results may be more variable for other elements; there were increasing concentrations of Mn due to microbial activity visible only for CHA colloids, and barely any or no "biotic" effect detected for As and Cr. In addition, the release of elements appears to be impacted by the type of bacteria even at similar pH conditions. Such a dependence on the type of bacteria may be explained by the diversity of the exudates produced, releasing organic ligands of different nature in different concentrations, as documented for soil

microorganisms under similar experimental conditions [40]. It could also be due to the nature of the tested bacteria. In this study we used two types of bacteria, Gram-positive (*Pseudomonas* sp.) and Gram-negative (*Mycolicibacterium* sp.) bacteria. It has been shown that Gram-positive bacteria absorb more humic acids and metallic elements in comparison with Gram-negative bacteria [58,59].

The dynamic of the release of metal(loid)s as a function of time (over 9 days) varies greatly from one element to another as well; there could be a regular increase in the solution with time (Fe, Pb), and in some cases there could be a decreasing concentration after six days (e.g., Mn and As for CHA colloids). Such different behaviors may suggest the presence of these elements under various forms that are more or less accessible to bacteria (e.g., adsorbed species, amorphous or refractory crystalline forms) and/or possible immobilization processes (e.g., adsorption, the precipitation of secondary phases). For Mn in CHA colloid incubations in particular, the decrease in concentration was only observed in biotic experiments, implying the role of micro-organisms in the immobilization of metals as well as in their release in the solution. Such behavior may be induced by many processes such as bio-precipitation or bio-sorption, among others [15], or also by the fact that Mn is highly sensitive to Eh/pH variations, inducing various speciations. It cannot be excluded that the other elements studied here were also involved in sorption or precipitation reactions, even those for which aqueous concentrations did not reveal any effect of the presence of bacteria in the system. Therefore, the bio-weathering effect described here is only partial and may involve greater quantities of elements. Further studies may focus on the speciation of the solid at the end of the bio-weathering experiments to assess the possible changes of the solid phase. In order to better predict the fate of the elements released in the aqueous compartments, it will be necessary to improve the characterization of the solid phases, both prior and after bio-weathering experiments, and to further study metal speciation and the reactivity of associated soluble organic compounds.

5. Conclusions

Surface sediments deposited in the bottom of LSC and CHA reservoirs have a strong potential to release nutrients (e.g., P) and potentially toxic elements (e.g., Pb, As) in colloidal form upon resuspension. The predominant fraction-carrying nutrients and metallic contaminants were large colloids (0.2–1 µm). The percentages of elements released with large colloids compared to the total amount contained in LSC and CHA sediments were, respectively, 3.6% and 18% for P, 2.3% and 2.7% for Al, 1.2% and 1.3% for Fe, 1.2% and 2.1% for Cr, 2.7% and 2.1% for Pb, and 1.1% and 1.2% for As. Our results also indicate that the fraction below 0.2 µm (operationally considered as dissolved) contain the colloids and nano-colloids (<100 nm). This highlights that the studied sediments contain a highly mobile colloidal fraction, which may be a significant contributor to the potential mobilization of nutrients and metallic elements from sediments to the water column. Thus, the release of the studied elements upon sediment resuspension may be a critical factor in controlling water quality.

The results demonstrated that under the experimental conditions (poor in nutrients, depleted in dissolved iron), both tested bacteria (*Pseudomonas* sp. and *Mycolicibacterium* sp.) were able to trigger nutrients from colloids (<1 µm) to maintain their growth. However, nutrient uptake from colloids was also involved in the release of colloid-bound contaminants into water (e.g., Pb, As). These first results are of great interest for the understanding of the mobility of metallic contaminants in surface aquatic systems. Indeed, the sediment fraction studied here, i.e., the water-dispersible colloids (submicrometric size fraction), represents the most chemically reactive interface in the transfer between biological–water–sediments reservoirs. This shows that dam reservoir systems could be viewed as large natural bioreactors. Furthermore, it seems essential to introduce the (micro-)biological factors to properly model the dynamics of the elements in those systems. Moreover, even if this study is focused on metallic elements, this bio-weathering effect may be important in other cycles of high interest for the management of large continental water bodies, e.g.,

the cycling of phosphorous and the effect on eutrophication. These results contribute to improving our understanding of the processes that influence contaminants' mobility in the ecosystems as well as providing an important insight into current research evaluating the bioavailability of different forms of nutrients.

Supplementary Materials: The following supporting information can be downloaded at: https://www.mdpi.com/article/10.3390/min12070812/s1, Figure S1: Grain size distribution of L'Escourou and Chamsanglard sediments.; Figure S2: Kinetics of carbohydrates consumption; Table S1: Major and trace elements composition of Champsanglard (CHA) and L'Escourou (LSC) sediments.; Table S2: Data for bulk sediments from Laser Diffraction measurements; Table S3: Chemical composition of the 0.2–1 µm size fraction of the colloids.

Author Contributions: Conceptualization, M.G. and V.R.; methodology, M.G.; validation, M.G. and V.R.; formal analysis, P.G., M.G. and V.R.; investigation, M.G., P.G., D.M., V.R., N.M., F.D. and P.F.; writing—original draft preparation, M.G. and V.R.; writing—review and editing, M.G., P.G., D.M., V.R., N.M., F.D., P.F. and E.J.; supervision, M.G. and V.R.; funding acquisition, E.J. and V.R. All authors have read and agreed to the published version of the manuscript.

Funding: Part of this research was funded by Region Nouvelle-Aquitaine, France ("MobiMet" project, AAP ESR 2020).

Conflicts of Interest: The authors declare no conflict of interest.

References

1. Kristensen, P.; Whalley, C.; Zal, F.N.N.; Christiansen, T. European Waters Assessment of Status and Pressures 2018. *EEA Rep.* **2018**, *7*, 85.
2. Jeppesen, E.; Søndergaard, M.; Jensen, J.P.; Havens, K.E.; Anneville, O.; Carvalho, L.; Coveney, M.F.; Deneke, R.; Dokulil, M.T.; Foy, B. Lake Responses to Reduced Nutrient Loading—An Analysis of Contemporary Long-term Data from 35 Case Studies. *Freshw. Biol.* **2005**, *50*, 1747–1771. [CrossRef]
3. Søndergaard, M.; Jeppesen, E.; Lauridsen, T.L.; Skov, C.; Van Nes, E.H.; Roijackers, R.; Lammens, E.; Portielje, R. Lake Restoration: Successes, Failures and Long-term Effects. *J. Appl. Ecol.* **2007**, *44*, 1095–1105. [CrossRef]
4. Søndergaard, M.; Jensen, J.P.; Jeppesen, E. Role of Sediment and Internal Loading of Phosphorus in Shallow Lakes. *Hydrobiologia* **2003**, *506*, 135–145. [CrossRef]
5. Schroeder, H.; Duester, L.; Fabricius, A.-L.; Ecker, D.; Breitung, V.; Ternes, T.A. Sediment Water (Interface) Mobility of Metal(Loid)s and Nutrients under Undisturbed Conditions and during Resuspension. *J. Hazard. Mater.* **2020**, *394*, 122543. [CrossRef]
6. Maavara, T.; Chen, Q.; Van Meter, K.; Brown, L.E.; Zhang, J.; Ni, J.; Zarfl, C. River Dam Impacts on Biogeochemical Cycling. *Nat. Rev. Earth Environ.* **2020**, *1*, 103–116. [CrossRef]
7. Frémion, F.; Courtin-Nomade, A.; Bordas, F.; Lenain, J.-F.; Jugé, P.; Kestens, T.; Mourier, B. Impact of Sediments Resuspension on Metal Solubilization and Water Quality during Recurrent Reservoir Sluicing Management. *Sci. Total Environ.* **2016**, *562*, 201–215. [CrossRef]
8. Nguyen, N.D.; Grybos, M.; Rabiet, M.; Deluchat, V. Spatial Distribution of Water-Mobilizable Colloids and Phosphorus from Dam Reservoir Sediment. In Proceedings of the Copernicus Meetings, Virtual, 19–30 April 2021.
9. Lead, J.R.; Wilkinson, K.J. Aquatic Colloids and Nanoparticles: Current Knowledge and Future Trends. *Environ. Chem.* **2006**, *3*, 159–171. [CrossRef]
10. Xu, H.; Ji, L.; Kong, M.; Xu, M.; Lv, X. Abundance, Chemical Composition and Lead Adsorption Properties of Sedimentary Colloids in a Eutrophic Shallow Lake. *Chemosphere* **2019**, *218*, 534–539. [CrossRef]
11. Nguyen, D.N.; Grybos, M.; Rabiet, M.; Deluchat, V. How Do Colloid Separation and Sediment Storage Methods Affect Water-Mobilizable Colloids and Phosphorus? An Insight into Dam Reservoir Sediment. *Colloids Surf. A: Physicochem. Eng. Asp.* **2020**, *606*, 125505. [CrossRef]
12. Saeed, H.; Hartland, A.; Lehto, N.; Baalousha, M.; Sikder, M.; Sandwell, D.; Mucalo, M.; Hamilton, D.P. Regulation of Phosphorus Bioavailability by Iron Nanoparticles in a Monomictic Lake. *Sci. Rep.* **2018**, *8*, 17736. [PubMed]
13. Eggleton, J.; Thomas, K.V. A Review of Factors Affecting the Release and Bioavailability of Contaminants during Sediment Disturbance Events. *Environ. Int.* **2004**, *30*, 973–980. [CrossRef] [PubMed]
14. Frémion, F.; Mourier, B.; Courtin-Nomade, A.; Lenain, J.-F.; Annouri, A.; Fondanèche, P.; Hak, T.; Bordas, F. Key Parameters Influencing Metallic Element Mobility Associated with Sediments in a Daily-Managed Reservoir. *Sci. Total Environ.* **2017**, *605–606*, 666–676. [CrossRef]
15. Sun, W.; Cheng, K.; Sun, K.Y.; Ma, X. Microbially Mediated Remediation of Contaminated Sediments by Heavy Metals: A Critical Review. *Curr. Pollut. Rep.* **2021**, *7*, 201–212.
16. Gu, Y.-G. Heavy Metal Fractionation and Ecological Risk Implications in the Intertidal Surface Sediments of Zhelin Bay, South China. *Mar. Pollut. Bull.* **2018**, *129*, 905–912.

17. Ren, J.; Williams, P.N.; Luo, J.; Ma, H.; Wang, X. Sediment Metal Bioavailability in Lake Taihu, China: Evaluation of Sequential Extraction, DGT, and PBET Techniques. *Environ. Sci. Pollut. Res.* **2015**, *22*, 12919–12928.
18. Cortada, U.; Hidalgo, M.C.; Martínez, J.; de la Torre, M.J. Mobility and Bioavailability of Metal(Loid)s in a Fluvial System Affected by the Mining and Industrial Processing of Pb. *Geosciences* **2021**, *11*, 167. [CrossRef]
19. Zhang, C.; Ding, S.; Xu, D.; Tang, Y.; Wong, M.H. Bioavailability Assessment of Phosphorus and Metals in Soils and Sediments: A Review of Diffusive Gradients in Thin Films (DGT). *Environ. Monit. Assess.* **2014**, *186*, 7367–7378. [CrossRef]
20. Lei, K.; Han, X.; Zhao, J.; Qiao, F.; Li, Z.; Yu, T. Characterization of Metal Kinetics and Bioavailability Using Diffusive Gradients in Thin Films Technique in Sediments of Taihu Lake, China. *Ecotoxicol. Environ. Saf.* **2016**, *128*, 153–160. [CrossRef]
21. Gu, Y.-G. Risk Assessment of Eight Metals and Their Mixtures to Aquatic Biota in Sediments with Diffusive Gradients in Thin Films (DGT): A Case Study in Pearl River Intertidal Zone. *Environ. Sci. Eur.* **2021**, *33*, 122. [CrossRef]
22. Ikem, A.; Egiebor, N.; Nyavor, K. Trace Elements in Water, Fish and Sediment from Tuskegee Lake, Southeastern USA. *Water Air Soil Pollut.* **2003**, *149*, 51–75. [CrossRef]
23. Grybos, M.; Billard, P.; Desobry-Banon, S.; Michot, L.J.; Lenain, J.-F.; Mustin, C. Bio-Dissolution of Colloidal-Size Clay Minerals Entrapped in Microporous Silica Gels. *J. Colloid. Interface Sci.* **2011**, *362*, 317–324. [CrossRef] [PubMed]
24. Murphy, J.; Riley, J.P. A Modified Single Solution Method for the Determination of Phosphate in Natural Waters. *Anal. Chim. Acta* **1962**, *27*, 31–36. [CrossRef]
25. Ruban, V.; López-Sánchez, J.; Pardo, P.; Rauret, G.; Muntau, H.; Quevauviller, P. Harmonized Protocol and Certified Reference Material for the Determination of Extractable Contents of Phosphorus in Freshwater Sediments–A Synthesis of Recent Works. *Fresenius J. Anal. Chem.* **2001**, *370*, 224–228. [CrossRef] [PubMed]
26. United States Environmental Protection Agency. *Determination of Phosphorus by Semi-Automated Colorimetry, Revision 2.0*; USEPA Method 365.1; United States Environmental Protection Agency: Washington, DC, USA, 1993.
27. DuBois, M.; Gilles, K.A.; Hamilton, J.K.; Rebers, P.A.; Smith, F. Colorimetric Method for Determination of Sugars and Related Substances. *Anal. Chem.* **1956**, *28*, 350–356. [CrossRef]
28. Chen, W.; Westerhoff, P.; Leenheer, J.A.; Booksh, K. Fluorescence Excitation−Emission Matrix Regional Integration to Quantify Spectra for Dissolved Organic Matter. *Environ. Sci. Technol.* **2003**, *37*, 5701–5710. [CrossRef] [PubMed]
29. Li, L.; Wang, Y.; Zhang, W.; Yu, S.; Wang, X.; Gao, N. New Advances in Fluorescence Excitation-Emission Matrix Spectroscopy for the Characterization of Dissolved Organic Matter in Drinking Water Treatment: A Review. *Chem. Eng. J.* **2020**, *381*, 122676. [CrossRef]
30. Kondolf, G.M.; Gao, Y.; Annandale, G.W.; Morris, G.L.; Jiang, E.; Zhang, J.; Cao, Y.; Carling, P.; Fu, K.; Guo, Q.; et al. Sustainable Sediment Management in Reservoirs and Regulated Rivers: Experiences from Five Continents. *Earths Future* **2014**, *2*, 256–280. [CrossRef]
31. Guo, X.; Zhu, X.; Yang, Z.; Ma, J.; Xiao, S.; Ji, D.; Liu, D. Impacts of Cascade Reservoirs on the Longitudinal Variability of Fine Sediment Characteristics: A Case Study of the Lancang and Nu Rivers. *J. Hydrol.* **2020**, *581*, 124343. [CrossRef]
32. Rapin, A.; Rabiet, M.; Mourier, B.; Grybos, M.; Deluchat, V. Sedimentary Phosphorus Accumulation and Distribution in the Continuum of Three Cascade Dams (Creuse River, France). *Environ. Sci. Pollut. Res.* **2020**, *27*, 6526–6539. [CrossRef]
33. Mahmood, Q.; Khan, A.F.; Khan, A. Chapter 25—Colloids in the Environmental Protection—Current and Future Trends. In *The Role of Colloidal Systems in Environmental Protection*; Fanun, M., Ed.; Elsevier: Amsterdam, The Netherlands, 2014; pp. 635–677. ISBN 978-0-444-63283-8.
34. Kretzschmar, R.; Barmettler, K.; Grolimund, D.; Yan, Y.; Borkovec, M.; Sticher, H. Experimental Determination of Colloid Deposition Rates and Collision Efficiencies in Natural Porous Media. *Water Resour. Res.* **1997**, *33*, 1129–1137. [CrossRef]
35. Kaplan, D.I.; Sumner, M.E.; Bertsch, P.M.; Adriano, D.C. Chemical Conditions Conducive to the Release of Mobile Colloids from Ultisol Profiles. *Soil Sci. Soc. Am. J.* **1996**, *60*, 269–274. [CrossRef]
36. Klitzke, S.; Lang, F.; Kaupenjohann, M. Increasing PH Releases Colloidal Lead in a Highly Contaminated Forest Soil. *Eur. J. Soil Sci.* **2008**, *59*, 265–273. [CrossRef]
37. Sun, Y.; Pan, D.; Wei, X.; Xian, D.; Wang, P.; Hou, J.; Xu, Z.; Liu, C.; Wu, W. Insight into the Stability and Correlated Transport of Kaolinite Colloid: Effect of PH, Electrolytes and Humic Substances. *Environ. Pollut.* **2020**, *266*, 115189. [CrossRef] [PubMed]
38. Maximova, N.; Dahl, O. Environmental Implications of Aggregation Phenomena: Current Understanding. *Curr. Opin. Colloid. Interface Sci.* **2006**, *11*, 246–266. [CrossRef]
39. Parrello, D.; Zegeye, A.; Mustin, C.; Billard, P. Siderophore-Mediated Iron Dissolution from Nontronites Is Controlled by Mineral Cristallochemistry. *Front. Microbiol.* **2016**, *7*, 423. [CrossRef]
40. Oulkadi, D.; Balland-Bolou-Bi, C.; Billard, P.; Kitzinger, G.; Parrello, D.; Mustin, C.; Banon, S. Interactions of Three Soil Bacteria Species with Phyllosilicate Surfaces in Hybrid Silica Gels. *FEMS Microbiol. Lett.* **2014**, *354*, 37–45. [CrossRef]
41. Fischer, H.; Wanner, S.C.; Pusch, M. Bacterial Abundance and Production in River Sediments as Related to the Biochemical Composition of Particulate Organic Matter (POM). *Biogeochemistry* **2002**, *61*, 37–55. [CrossRef]
42. Haglund, A.-L.; Törnblom, E.; Boström, B.; Tranvik, L. Large Differences in the Fraction of Active Bacteria in Plankton, Sediments, and Biofilm. *Microb. Ecol.* **2002**, *43*, 232–241. [CrossRef]
43. Haglund, A.-L.; Lantz, P.; Törnblom, E.; Tranvik, L. Depth Distribution of Active Bacteria and Bacterial Activity in Lake Sediment. *FEMS Microb. Ecol.* **2003**, *46*, 31–38. [CrossRef]

44. Pachepsky, Y.; Shelton, D. Escherichia Coli and Fecal Coliforms in Freshwater and Estuarine Sediments. *Crit. Rev. Environ. Sci. Technol.* **2011**, *41*, 1067–1110. [CrossRef]
45. Goulder, R. Attached and Free Bacteria in an Estuary with Abundant Suspended Solids. *J. Appl. Bacteriol.* **1977**, *43*, 399–405. [CrossRef]
46. Guber, A.K.; Pachepsky, Y.A.; Shelton, D.R.; Yu, O. Effect of Bovine Manure on Fecal Coliform Attachment to Soil and Soil Particles of Different Sizes. *Appl. Environ. Microbiol.* **2007**, *73*, 3363–3370. [CrossRef]
47. Wu, T.; Zhai, C.; Zhang, J.; Zhu, D.; Zhao, K.; Chen, Y. Study on the Attachment of Escherichia Coli to Sediment Particles at a Single-Cell Level: The Effect of Particle Size. *Water* **2019**, *11*, 819. [CrossRef]
48. Meunier, C.F.; Dandoy, P.; Su, B.-L. Encapsulation of Cells within Silica Matrixes: Towards a New Advance in the Conception of Living Hybrid Materials. *J. Colloid. Interface Sci.* **2010**, *342*, 211–224. [CrossRef] [PubMed]
49. Kalinowski, B.E.; Liermann, L.J.; Givens, S.; Brantley, S.L. Rates of Bacteria-Promoted Solubilization of Fe from Minerals: A Review of Problems and Approaches. *Chem. Geol.* **2000**, *169*, 357–370. [CrossRef]
50. Hider, R.C.; Kong, X. Chemistry and Biology of Siderophores. *Nat. Prod. Rep.* **2010**, *27*, 637. [CrossRef]
51. Rogers, J.R.; Bennett, P.C. Mineral Stimulation of Subsurface Microorganisms: Release of Limiting Nutrients from Silicates. *Chem. Geol.* **2004**, *203*, 91–108. [CrossRef]
52. Hersman, L.; Lloyd, T.; Sposito, G. Siderophore-Promoted Dissolution of Hematite. *Geochim. Cosmochim. Acta* **1995**, *59*, 3327–3330. [CrossRef]
53. Oulkadi, D.; Balland-Bolou-Bi, C.; Michot, L.J.; Grybos, M.; Billard, P.; Mustin, C.; Banon, S. Bioweathering of Nontronite Colloids in Hybrid Silica Gel: Implications for Iron Mobilization. *J. Appl. Microbiol.* **2014**, *116*, 325–334. [CrossRef]
54. Saha, R.; Saha, N.; Donofrio, R.S.; Bestervelt, L.L. Microbial Siderophores: A Mini Review. *J. Basic Microbiol.* **2013**, *53*, 303–317. [CrossRef] [PubMed]
55. Perez, A.; Rossano, S.; Trcera, N.; Verney-Carron, A.; Rommevaux, C.; Fourdrin, C.; Agnello, A.C.; Huguenot, D.; Guyot, F. Direct and Indirect Impact of the Bacterial Strain Pseudomonas Aeruginosa on the Dissolution of Synthetic Fe(III)- and Fe(II)-Bearing Basaltic Glasses. *Chem. Geol.* **2019**, *523*, 9–18. [CrossRef]
56. Gottselig, N.; Nischwitz, V.; Meyn, T.; Amelung, W.; Bol, R.; Halle, C.; Vereecken, H.; Siemens, J.; Klumpp, E. Phosphorus Binding to Nanoparticles and Colloids in Forest Stream Waters. *Vadose Zone J.* **2017**, *16*, 1–12. [CrossRef]
57. Kumari, S.; Mahapatra, S.; Das, S. Ca-Alginate as a Support Matrix for Pb (II) Biosorption with Immobilized Biofilm Associated Extracellular Polymeric Substances of Pseudomonas Aeruginosa N6P6. *Chem. Eng. J.* **2017**, *328*, 556–566. [CrossRef]
58. Mullen, M.; Wolf, D.; Ferris, F.; Beveridge, T.; Flemming, C.; Bailey, G. Bacterial Sorption of Heavy Metals. *Appl. Environ. Microbiol.* **1989**, *55*, 3143–3149. [CrossRef] [PubMed]
59. Tikhonov, V.; Drozdova, O.; Cheptsov, V.; Demin, V. Sorption of Dissolved Organic Matter by Freshwater Bacterioplankton. EDP Sciences. In Proceedings of the E3S Web of Conferences, Virtual, 3 June 2021; Volume 265.